Ranah Research
Journal of Multidisciplinary Research and Development
E-ISSN: 2655-0865
DINASTI RESEARCH
082170743613 ranahresearch@gmail.com https://jurnal.ranahresearch.com

DOI: https://doi.org/10.38035/rrj.v8i6

Segment-Based DWDM Lightpath Monitoring Using an Interval Type-2 Fuzzy Logic System and Temporal Stabilization

Riya Wahyudi[1], Andi Adriansyah[2]
[1]Master's Program in Electrical Engineering, Mercu Buana University, Jakarta, Indonesia
[2]Master's Program in Electrical Engineering, Mercu Buana University, Jakarta, Indonesia

Corresponding Author: 55422110001@student.mercubuana.ac.id[1]

Abstract: Optical protection switching on dynamic IS-IS and MPLS backbones can trigger adjacency resets, producing false positives and alarm flapping. This study designs a DWDM lightpath monitoring system using an Interval Type-2 Fuzzy Logic System (IT2FLS) as the alarm classifier, combined with a temporal stabilizer of debounce N=3 and hold-down H=3 to suppress false alarms. Data were collected through ICMP active probing from Customer Edge devices with strict path locking, yielding 736,764 samples from 34 lightpaths over 144 hours. The stabilizer reduced total alarm events from 6,333 to 2,313 (down 63.5%) and the false positive rate from 13.33 to 5.08 per hour (down 61.9%), with recall remaining high at 0.921 despite a decrease from 0.986 under raw conditions. The stabilizer effect was significant and consistent across the 34 segments (Wilcoxon signed-rank, $p < 10^{-6}$). The system is proven to suppress false alarms without changing the total reported fault duration.

Keywords: Alarm Management, DWDM, Interval Type-2 Fuzzy Logic, MPLS TE.

INTRODUCTION

Traffic volume has been doubling approximately every one to two years (Xie & Zhang, 2022). Internet Service Providers (ISPs) use Dense Wavelength Division Multiplexing (DWDM)-based optical transport networks as intercity backbones to carry this traffic volume, including supporting 5G and subsequent generations of mobile networks (Manias et al., 2023). In Indonesia, operators have modernized DWDM equipment on intercity backbone routes to increase channel capacity and maintain network performance (Simanjuntak et al., 2022). To maximize resource utilization, networks are operated with tight margins. This condition increases the risk of severe failures and necessitates an accurate early-warning detection system (Cruzes, 2024).

Modern ISP backbones form a two-layer architecture. At the logical layer, Intermediate System to Intermediate System (IS-IS) and Multiprotocol Label Switching (MPLS) function as an overlay that defines links between routers (Mayr et al., 2021). At the physical layer, DWDM acts as an underlay that carries each of these links as a lightpath with working and protection path configurations (Klinkowski, 2024). The protection path is calculated as a link-disjoint path from the working path to ensure resilience against single-link failures (Kim, 2024). When an optical fiber on the primary path is disrupted, DWDM performs Optical Protection Switching

(OPS) to the protection path within approximately 50 ms (Figueroa-García et al., 2023). Under seamless switching conditions, IS-IS does not detect this event because the logical link remains UP and the adjacency status does not change (Edozie et al., 2025). However, the protection path is generally longer, causing the event to manifest as a persistent increase in latency. Under non-seamless switching conditions, the IS-IS adjacency temporarily changes state, and the dynamic IS-IS protocol immediately recalculates the routing paths (Zhao et al., 2024), causing packets traversing the affected link to be temporarily redirected to alternative links (Reyes et al., 2021). Without path pinning, probe packets are also rerouted, resulting in the loss of reference to the monitored lightpath.

This measurement inconsistency generates false positives and alarm flapping, which burden Network Operations Center (NOC) operators and reduce confidence in the monitoring system (Andrade et al., 2022). Existing approaches remain fragmented. Rule-based alarm suppression applies uniform thresholds without considering the characteristics of individual segments (Li et al., 2023). Fuzzy-based service quality classification uses a single global parameter and therefore fails to distinguish between intra-city and intercity lightpaths (Kh Altmemi et al., 2022). Machine learning-based failure management can achieve high accuracy but is difficult to interpret and trace (Chen et al., 2022). Meanwhile, the application of Interval Type-2 Fuzzy Logic Systems (IT2FLS) to inter-segment optical network monitoring has generally not exploited an adaptive Footprint of Uncertainty (FOU) structure. Dynamic FOU structures have been proposed in other domains, such as quadcopter altitude control (Şahin & Ulu, 2023), but their application to inter-segment lightpath performance classification remains unexplored. In contrast to these studies, this research integrates path pinning, IT2FLS classification with segment-specific FOU profiles, and temporal stabilization into a single external monitoring framework evaluated using real-world intercity DWDM lightpath data.

In this study, the authors propose a DWDM lightpath performance monitoring system that operates externally through active ICMP probing from Customer Edge (CE) devices located at the nearest Point of Presence (POP), without requiring access to the operator's core network equipment. Path pinning is implemented using a Layer 2 VPN service layer and MPLS Traffic Engineering configured with a strict path, ensuring that probe packets consistently traverse the same lightpath even when IS-IS performs rerouting. Latency and packet loss performance are classified using an IT2FLS with segment-specific FOU profiles calibrated for each segment and subsequently stabilized using debounce N=3 and hold-down H=3 mechanisms, along with deterministic rules for link-down conditions (100% packet loss). These mechanisms suppress false positives and alarm flapping at the decision layer.

Accordingly, the proposed system improves the accuracy and stability of alarm decisions without altering the underlying latency or packet loss values, which are outside the scope of this study, thereby enabling NOC operators to isolate faults more rapidly. The primary novelty lies in the segment-specific FOU profiles, which adapt the concept of dynamic FOU to the context of inter-segment lightpath performance classification an application that has not been addressed in previous IT2FLS literature. Therefore, this approach has the potential to be adopted by other operators facing similar challenges.

METHODS

Research Design

This study employed an engineering research methodology based on a prototype-oriented design to develop an intelligent monitoring system for DWDM backbone lightpath performance. The proposed framework integrates three principal components: ICMP active probing with MPLS Traffic Engineering strict-path routing for deterministic network measurement, an Interval Type-2 Fuzzy Logic System (IT2FLS) with segment-specific Footprint of Uncertainty (FOU) profiles for adaptive alarm classification, and temporal stabilization mechanisms combined with deterministic rules to reduce false alarms and alarm

flapping. The conceptual position of the proposed approach within the existing body of knowledge is illustrated in Figure 1, demonstrating the integration of network performance measurement, intelligent fuzzy inference, and alarm stabilization into a unified monitoring architecture. Finally, a scenario-based comparative evaluation framework was designed to systematically quantify the individual and combined contributions of these components to improving alarm quality, classification reliability, and monitoring performance.

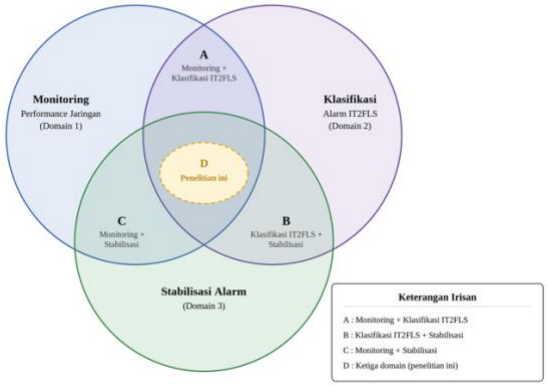

Figure 1. Venn Diagram Illustrating the Position of the Research

Research Object and Dataset Characteristics

Table 1. Summary of Monitored Lightpaths (34 Segments)

Originating City	Number	Destination City	Target IP Subnet	Baseline (ms)	API Access
Jakarta (Tebet)	5	Cirebon, Bandung, Semarang, Surabaya, Malang	10.26.100.0/24	6–15	CE TEBET
Jakarta (Duren Tiga)	6	Cirebon, Bandung, Semarang, Solo, Surabaya, Malang	10.26.101.0/24	6–15	CE TEBET
Jakarta (Cyber)	5	Bandung, Semarang, Solo, Surabaya, Malang	10.26.102.0/24	6–15	CE TEBET
Cirebon	2	Garut, Tasikmalaya	10.26.103.0/24	3	CE CIREBON
Bandung	2	Garut, Tasikmalaya	10.26.104.0/24	1–2	CE BANDUNG
Semarang	3	Salatiga, Klaten, Yogyakarta	10.26.105.0/24	1–2	CE SEMARANG
Solo	3	Salatiga, Klaten, Yogyakarta	10.26.106.0/24	1	CE SOLO
Surabaya	4	Kediri, Lumajang, Probolinggo, Banyuwangi	10.26.107.0/24	2–4	CE SURABAYA
Malang	4	Kediri, Lumajang, Probolinggo, Banyuwangi	10.26.108.0/24	1–5	CE MALANG

Table 1 presents the monitoring configuration of 34 DWDM backbone lightpath segments distributed across nine originating cities and multiple regional destinations in Indonesia, providing the experimental dataset used throughout this study. Each monitored segment is associated with a dedicated target IP subnet, Customer Edge (CE) API access point, and baseline latency profile ranging from 1 to 15 ms, representing the expected transmission characteristics of different intercity and inner-city lightpaths. Standardized ICMP probing was performed across all segments to collect real-time latency and packet loss measurements under a consistent monitoring framework, thereby ensuring comparable observations throughout the network. This structured dataset establishes a reliable foundation for subsequent performance evaluation, intelligent alarm classification, and comparative analysis of the proposed monitoring system.

Prototype System Architecture

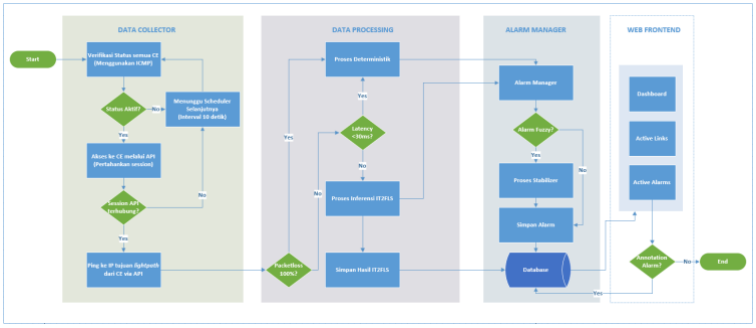

Figure 2. Monitoring System Design

The proposed monitoring prototype was developed as an end-to-end modular pipeline that separates the processes of data acquisition, intelligent processing, alarm management, data storage, and information visualization to improve system scalability, maintainability, and operational efficiency. As illustrated in Figure 2, the Data Collector module continuously verifies the availability of Customer Edge (CE) devices through ICMP communication, establishes API sessions, and executes active ICMP probes to each monitored IP address for real-time network performance measurement. The collected measurements are subsequently processed by the Data Processing module, which integrates deterministic decision rules with Interval Type-2 Fuzzy Logic System (IT2FLS) inference to classify network conditions, while the Alarm Manager applies debounce and hold-down mechanisms to suppress alarm flapping and records validated events in the *alarm_history* database. Finally, all monitoring data are centrally maintained in the Database, and the Web Frontend provides interactive dashboards that enable network operators to visualize real-time performance metrics, alarm status, and historical events for comprehensive monitoring and operational decision-makin.

Measurement Protocol and Data Preprocessing

Measurement consistency was ensured through ICMP active probing over MPLS Traffic Engineering configured with a strict path, preventing probe rerouting during temporary IS-IS adjacency changes and enabling packet loss to accurately reflect network disruptions while maintaining low operational overhead compared with TWAMP and Y.1731 OAM (Kim, 2024; Miranda et al., 2022; Amjad et al., 2021). Active ICMP Echo measurements were performed using fixed parameters, including a nominal 10-second polling interval, five packets per cycle, median round-trip time (RTT) for latency estimation, and packet loss percentage, in accordance with the QoS performance recommendations of ITU-T Y.1540 and ITU-T Y.1541 Before analysis, the collected time-series data were reconstructed on a segment-based temporal grid, explicitly distinguishing unreachable conditions from missing observations to ensure measurement accountability and reproducibility. The decision engine was implemented using an Interval Type-2 Fuzzy Logic System (IT2FLS) comprising a fuzzifier, rule base, inference engine, type-reducer, and defuzzifier, with fuzzy knowledge represented according to IEEE Std 1855-2016 Fuzzy Markup Language (Wu & Mendel, 2019; IEEE, 2016).

Classification Engine (IT2FLS)

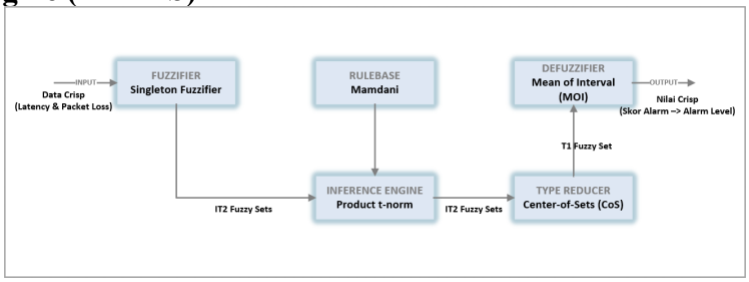

Figure 3. IT2FLS System Design

Table 2. Mamdani Rule Base of 16 Rules (Status Consequents for Each Input Combination)

Latency \ Packet Loss	Normal	Slightly Increased	Moderately Increased	Highly Increased
Normal	Normal	Warning	Average	Critical
Slightly Increased	Warning	Warning	Average	Critical
Moderately Increased	Average	Average	Average	Critical
Highly Increased	Critical	Critical	Critical	Critical

The proposed classification engine employs an Interval Type-2 Fuzzy Logic System (IT2FLS), consisting of a singleton fuzzifier, a 16-rule Mamdani rule base (Table 2), an inference engine, a Center-of-Sets (CoS) type-reducer, and a Mean of Interval (MOI) defuzzifier (Figure 3), where latency and packet loss are represented by trapezoidal Upper Membership Functions (UMF) and Lower Membership Functions (LMF) with segment-specific Footprints of Uncertainty (FOU) for latency and global profiles for packet loss (Wu & Mendel, 2019; IEEE, 2016). The inference engine computes the firing interval of each rule using the product t-norm,

$$\bar{f}_n = \mu_{\text{lat}}^{\text{UMF}}(x) \times \mu_{\text{pl}}^{\text{UMF}}(y),\ \underline{f}_n = \mu_{\text{lat}}^{\text{LMF}}(x) \times \mu_{\text{pl}}^{\text{LMF}}(y), \tag{1}$$

followed by Center-of-Sets type reduction,

$$y_l = \frac{\sum_{n=1}^{N} z_{l,n}\, w_{l,n}}{\sum_{n=1}^{N} w_{l,n}},\ y_r = \frac{\sum_{n=1}^{N} z_{u,n}\, w_{u,n}}{\sum_{n=1}^{N} w_{u,n}}, \tag{2}$$

to generate the Type-1 interval (Wu & Mendel, 2019). The final crisp output is obtained using the Mean of Interval,

$$y = \frac{y_l + y_r}{2}, \tag{3}$$

and is subsequently mapped into four alarm levels (Normal, Warning, Average, and Critical) according to predefined thresholds (Mendel, 2024). Finally, the generated alarm status is stored in the alarm_history database using a start–end event model, where each event is classified as either DEGRADATION or OUTAGE based on the detected fault type, thereby supporting event-level monitoring and subsequent performance evaluation.

Segment-Specific FOU Calibration & Baseline Validation

Table 3. Distribution of Baseline Profiles Across 34 Segments

Baseline (ms)	Number of Segments	Segments
1	5	Bandung–Garut, Solo–Klaten, Semarang–Salatiga
2	9	Malang–Kediri, Semarang–Klaten, Surabaya–Kediri
3	2	Cirebon–Garut, Surabaya–Lumajang
4	5	Cyber–Bandung, Tebet–Bandung, Malang–Banyuwangi
5	2	Duren Tiga–Cirebon, Tebet–Cirebon
10	3	Cyber–Semarang, Duren Tiga–Semarang, Tebet–Semarang
11	2	Cyber–Solo, Duren Tiga–Solo
12	1	Tebet–Surabaya
14	2	Cyber–Surabaya, Duren Tiga–Surabaya
15	3	Cyber–Malang, Duren Tiga–Malang, Tebet–Malang

The proposed system introduces segment-specific Footprint of Uncertainty (FOU) profiles by adapting latency membership functions to the baseline latency of each DWDM lightpath, enabling alarm classification to reflect the normal operating characteristics of individual segments instead of relying on a single global threshold. Fifteen baseline profiles ranging from 1 to 15 ms were assigned across the 34 monitored lightpath segments, as summarized in Table 3, thereby accommodating the heterogeneous latency characteristics of both inner-city and intercity backbone links. To validate the calibration, the configured baseline values were compared with the measured median round-trip time (RTT) over a one-week observation period by calculating the correlation coefficient and mean absolute error (MAE)

for all monitored segments, ensuring that the profiles accurately represented the physical characteristics of each lightpath before classification. This calibration strategy extends the adaptive FOU concept previously applied in dynamic control systems to optical network performance monitoring, thereby providing a novel approach for segment-level latency classification and fair alarm assessment across heterogeneous DWDM backbone networks (Şahin & Ulu, 2023).

Stabilization, Deterministic Rules, and Incident Logging

The proposed monitoring system employed a stateful stabilization mechanism to suppress alarm flapping by maintaining status memory for each monitored segment and applying an asymmetric debounce–hold-down strategy, where status transitions were confirmed only after N = 3 consecutive samples and alarm clearance required H = 3 persistent recovery samples, corresponding to an effective stabilization window of approximately 72 s. During active incidents, any changes in severity level (Normal = 0, Warning = 1, Average = 2, Critical = 3) or fault type automatically updated the recorded incident to ensure consistent event tracking and hysteresis-based alarm management. A deterministic fast-path rule was introduced to prioritize complete link failures, where packet loss was computed as:

$$PL = \frac{\text{sent} - \text{received}}{\text{sent}} \times 100\%;$$

consequently, when received = 0, PL = 100% and the corresponding RTT measurement was considered invalid, while phantom packet detection forced PL = 100% whenever PL ≥ 80% and RTT ≥ 900 ms to avoid false latency-induced alarms. Finally, any condition satisfying PL = 100% was immediately classified as Critical/OUTAGE before IT2FLS inference or threshold evaluation and subsequently verified through three consecutive observations to eliminate transient noise and improve incident reliability.

Experimental Setup and Performance Evaluation

Table 4. 2×2 Factorial Matrix of Testing Scenarios

	Threshold	IT2FLS
Without Stabilization	S1 – Raw Threshold	S2 – Raw IT2FLS
With Stabilization	S3 – Threshold + Stabilizer	S4 – IT2FLS + Stabilizer

The experimental evaluation was designed to verify four objectives: traceable segment-level monitoring, fully external ICMP-based operation without access to core network devices, IT2FLS-based alarm classification using latency and packet loss, and improved alarm coherence through stabilization. A 2 × 2 factorial design compared two classification methods (Threshold and IT2FLS) with and without stabilization, resulting in four testing scenarios (S1–S4), while an additional sensitivity analysis compared segment-specific FOU profiles against a global 4 ms baseline to assess the necessity of segment-level calibration. Alarm performance was assessed using event-based metrics, including the number of events (N), alarm rate (N/T_{obs}), where $T_{obs} = 144$hours, and the Short Alarm Ratio $(SAR_{<\tau})$with $\tau = 30$s, whereas persistent non-Normal conditions lasting at least 120 s (280 reference intervals) were treated as the ground-truth proxy for calculating precision, recall, F1-score, and false-positive rate, with true-positive events defined according to persistence overlap (Joshi & Garg, 2022). Finally, the statistical significance of the stabilization strategy and classification method was evaluated using the Wilcoxon signed-rank test across all 34 monitored segments to ensure that performance differences reflected consistent segment-level improvements rather than isolated anomalies (Rainio et al., 2024).

RESULTS AND DISCUSSION

This section presents the results of the prototype evaluation and the corresponding analysis. The system was developed using the Python programming language, with a pipeline consisting of a data collector module (ICMP active probing), a data processing module (deterministic decision-making and IT2FLS inference), an alarm manager module (debounce/hold-down), and a web frontend, supported by a centralized database. The evaluation was conducted using 144 hours of time-series data (31 May–6 June 2026) from 34 DWDM lightpaths, yielding 736,764 valid samples, as presented in Table 5. Four alarm outputs were compared using a 2×2 factorial design: threshold without stabilization (S1), IT2FLS without stabilization (S2), threshold with stabilization (S3), and IT2FLS with stabilization (S4). All conclusions were derived from measured values and further supported by statistical tests.

Table 5. Summary of Monitoring Results

Parameter	Value	Description
Number of DWDM lightpaths	34	As presented in Table 1
Observation Period	144 hours	31 May–6 June 2026
Total Valid Samples	736,764	monitoring_data
Effective Polling Cadence	≈ 24 seconds	Median interval between samples: 23.7 s
Unreachable Samples (PL 100%)	15,621	2.12% of total samples
Median avg_rtt (P90)	4.0 ms (≈ 13.9 ms)	Range: 0.7–55.4 ms
Uncleared Alarms	0	All events were closed

The system was implemented on a Virtual Machine (VM) server connected to a MikroTik router through an Application Programming Interface (API), which served as the Customer Edge (CE). The device secured the DWDM lightpath monitoring path using a Layer 2 MPLS VPN service, combined with MPLS Traffic Engineering (MPLS TE) path pinning on the ISP backbone, which operates over the IS-IS protocol. With this configuration, the monitored DWDM lightpaths were ensured to remain on the predefined pinned paths. The monitoring data were subsequently displayed on the dashboard, as shown in Figure 4.

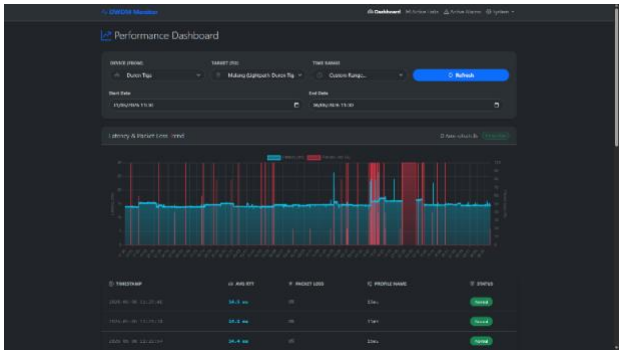

Figure 4. Monitoring System Prototype

The performance of the four scenarios was evaluated using data from alarm_history based on event-level metrics, including the number of events, alarm rate, and Short Alarm Ratio (SAR), as well as accuracy metrics against the persistence-based reference of ≥120 seconds across 280 actual degradation intervals, including precision, recall, F1-score, and false-positive rate. A summary of the performance is presented in Table 6 and visualized in Figure 5.

Table 6. Summary of Evaluation Results Across Scenarios S1–S4

Scenario	Events (N)	Rate (/hour)	SAR<30s	Precision	Recall	F1-Score	FP (/hour)
S1 (Raw Threshold)	6,362	44.18	0.564	0.695	0.986	0.815	13.47

Scenario	Events (N)	Rate (/hour)	SAR<30s	Precision	Recall	F1-Score	FP (/hour)
S2 (Raw IT2FLS)	6,333	43.98	0.565	0.697	0.986	0.816	13.33
S3 (Threshold + Stabilizer)	2,384	16.56	0.344	0.677	0.921	0.780	5.35
S4 (IT2FLS + Stabilizer)	2,313	16.06	0.342	0.684	0.921	0.785	5.08

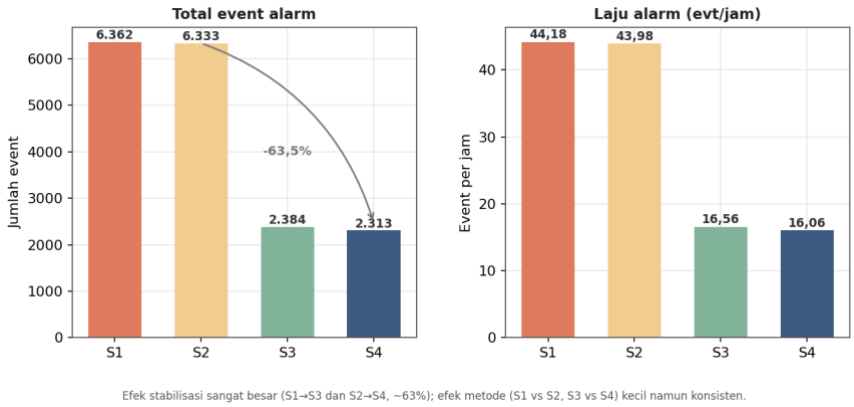

Figure 5. Comparison of Alarm Counts and Alarm Rates Across Scenarios

The application of the stabilizer substantially reduced the total number of events in both pipelines, from 6,333 to 2,313 in the IT2FLS pipeline (a 63.5% reduction) and from 6,362 to 2,384 in the threshold pipeline (a 62.5% reduction), with SAR<30s decreasing from 0.565 to 0.342. The median event duration increased from 25.0 to 53.7 seconds, while the total alarm duration remained nearly unchanged (approximately 643–645 hours), as shown in Figure 5. In contrast, the difference between the two methods (IT2FLS vs. threshold) was small in terms of the number of events.

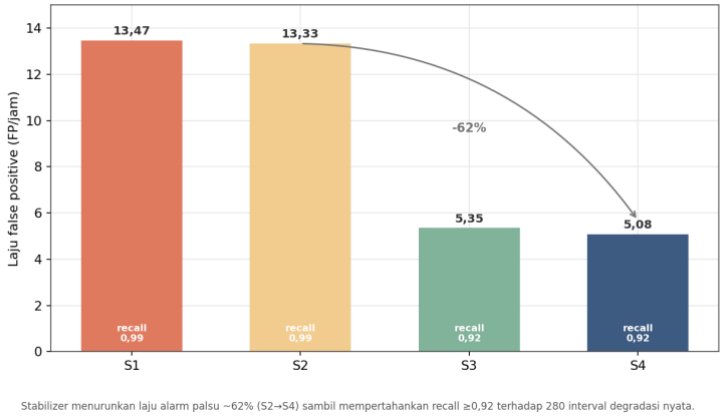

Figure 6. False-Positive Rate Across Scenarios (Persistence-Based Proxy ≥120 s)

In terms of accuracy, as shown in Figure 6, stabilization in the IT2FLS pipeline reduced the false-positive rate from 13.33 to 5.08 FP/hour (a 61.9% reduction), while recall remained high at 0.921 (down from 0.986 in the raw configuration). The system still detected more than 92% of actual degradations despite suppressing transient alarms. A similar pattern was observed in the threshold pipeline (13.47 → 5.35 FP/hour), with event-based precision remaining relatively stable (0.697 → 0.684). The Wilcoxon signed-rank test across the 34 segments confirmed that the stabilization effect was highly significant for both pipelines ($p < 10^{-6}$), with a median reduction in events per segment of 39.2%. In contrast, the method effect was small

and not statistically significant in the raw configurations (p = 0.383), but became statistically significant with a small effect size after stabilization (p = 0.014).

Table 7. Wilcoxon Signed-Rank Test on Segment-Level Metrics (n = 34)

Comparison	Metric	Median Reduction (IQR)	p-value
S2 vs. S4 (stabilization, IT2FLS)	Total Events	39.2% (25.1–56.6)	8.6×10^{-7}
S1 vs. S3 (stabilization, threshold)	Total Events	39.2% (21.3–54.8)	8.6×10^{-7}
S2 vs. S4 (stabilization, IT2FLS)	SAR<30s	0.166 (0.136–0.249)	9.3×10^{-10}
S1 vs. S3 (stabilization, threshold)	SAR<30s	0.161 (0.134–0.248)	8.7×10^{-7}
S3 vs. S4 (method, stabilized)	Total Events	Median Δ 2 events	0.014
S1 vs. S2 (method, raw)	Total Events	Median Δ 1.5 events	0.383 (n.s.)

The detailed test results are presented in Table 7, while the consistency of the reduction across segments is visualized in Figure 7. The reduction occurred across nearly all segments, with the most pronounced decreases observed in high-event segments such as Bandung–Garut (2,019 → 493 under IT2FLS) and Cirebon–Garut (978 → 190). These results indicate that the stabilizer effect was consistent across segments and was not driven by only a small number of problematic segments.

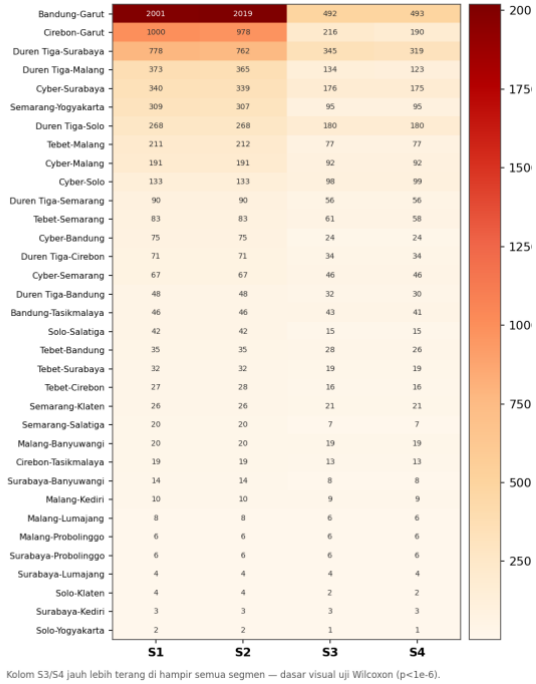

Figure 7. Heatmap of Event Counts by Segment × Scenario

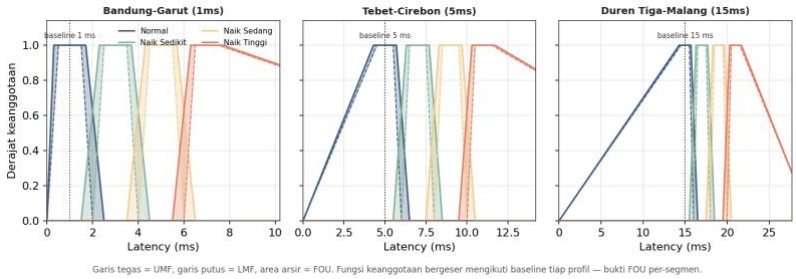

Figure 8. Segment-Specific FOU Profiles from the Actual System Configuration (Three Representative Segments)

The segment-specific FOU profiles were calibrated according to the latency baseline of each lightpath, as shown in Figure 8. Validation of the configured baselines against the

measured median RTT yielded a correlation coefficient of r = 0.995 and a mean absolute error of 0.40 ms, indicating that status assessment was performed relative to the physical characteristics of each segment. In the ablation study, for segments with high baselines (≥10 ms), the segment-specific profiles classified only 7.9% of samples as non-Normal, whereas a single global 4 ms profile classified all samples (100%) as non-Normal. This indicates that, without segment-specific calibration, 92.1% of normal traffic on intercity segments would be incorrectly flagged as alarms.

To demonstrate the system's behavior under real-world conditions, Figure 9 presents the latency time series and alarm status for the four scenarios on the Duren Tiga–Malang segment (baseline ≈15 ms) over a representative 12-hour observation window (4–5 June 2026).

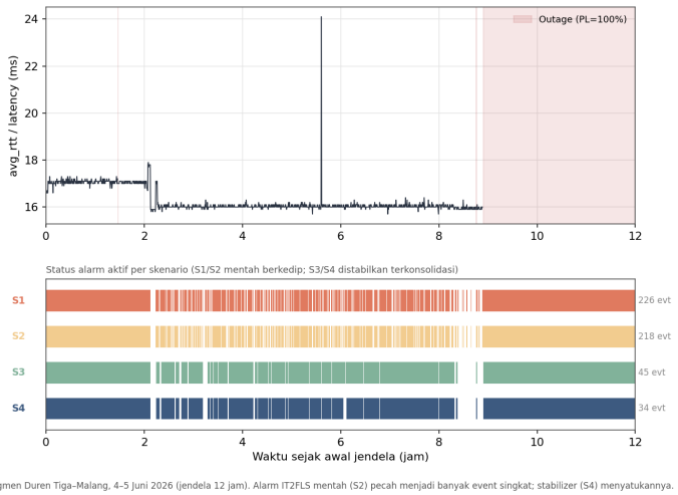

Figure 9. Latency Time Series and Alarm Status Across Four Scenarios (Duren Tiga–Malang)

Three characteristic events can be observed within this window: protection switching (a decrease in latency after the second hour), a single transient spike (around hour 5.6), and an unreachable condition (PL = 100%) at the end of the observation window. The raw alarm outputs (S1 and S2) fragmented into hundreds of short events as latency fluctuated, producing 226 and 218 events, respectively. In contrast, the stabilizer (S3 and S4) consolidated these into dozens of meaningful events (45 and 34 events, respectively) without missing the outage condition, which was handled by the deterministic fast-path rule.

Discussion

The substantial reduction in the number of events, accompanied by an almost unchanged total alarm duration, indicates that the stabilizer consolidated repeated short-lived events caused by flapping into a smaller number of events with reasonable durations, rather than randomly suppressing alarms. Meanwhile, the small difference between the methods in terms of event counts indicates that the largest practical contribution came from the stabilizer. Event-based precision remained relatively stable because the stabilizer consolidated both true-positive and false-positive events simultaneously. Therefore, the more relevant indicator of NOC workload is the absolute false-positive rate per hour, which decreased by 61.9%.

This reduction rate is comparable to the more than 62% reduction in redundant alarms reported by Li et al., (2023) using association mining. However, the temporal stabilizer proposed in this study operates proactively at the decision layer, suppressing flapping before alarms are generated, in contrast to reactive approaches based on trouble-ticket prediction (Adnan & Kumaravel, 2025). The Wilcoxon test results in Table 7 are also consistent with the findings of hybrid anomaly detection studies (Chen et al., 2022), which suggest that individual components require structural enhancement or explicit rules to achieve stability in high-risk

cases. Accordingly, the most practically relevant configuration is the final S4 model, which combines adaptive IT2FLS with temporal stabilization.

Based on the baseline validation results (r = 0.995) and the ablation study, the qualitative advantage of IT2FLS lies in its segment-specific FOU profiles, which serve as a prerequisite for fair classification across segments. This finding also extends the application of the adaptive FOU concept, previously explored in control domains such as quadcopter control (Şahin & Ulu, 2023), to optical network monitoring, a field that has been predominantly characterized by machine learning approaches (Wang et al., 2022), while maintaining traceable decision-making (Mendel, 2024).

The operational simulation presented in Figure 9 further demonstrates that the system is responsive and interpretable in a near-real-time monitoring context. Operators receive stable and traceable alarms rather than a flood of transient alarms, thereby reducing the triage workload at the NOC and potentially accelerating the isolation of intercity network faults (Andrade et al., 2022).

CONCLUSIONS AND RECOMMENDATIONS

This study demonstrates that a fully external DWDM lightpath performance monitoring system integrating MPLS Traffic Engineering strict-path routing, IT2FLS classification with segment-specific FOU profiles, and temporal stabilization can improve alarm quality on intercity backbones without requiring access to the operator's core network equipment. The greatest practical contribution comes from the temporal stabilizer, which reduced the number of alarm events by 63.5% (6,333 → 2,313) and the false-positive rate by 61.9% (13.33 → 5.08 FP/hour) in the IT2FLS pipeline, while recall remained high at 0.921 (down from 0.986 in the raw configuration), meaning that more than 92% of actual degradations were still detected. The stabilizer effect was statistically significant and consistent across all 34 segments, as confirmed by the Wilcoxon signed-rank test ($p < 10^{-6}$). Meanwhile, the segment-specific FOU profiles, validated against measured data (correlation r = 0.995), proved to be a prerequisite for fair classification across segments, as without segment-specific calibration, 92.1% of normal traffic on intercity segments would have been incorrectly flagged as alarms.

Accordingly, the final S4 system, which combines adaptive IT2FLS and temporal stabilization, provides the best balance between sensitivity to actual network disturbances and alarm stability while maintaining traceable decision-making. These findings are relevant to near-real-time monitoring and can help NOC operators reduce triage workloads and accelerate the isolation of intercity network faults. The main limitation is that alarm correctness was evaluated using a persistence-based ground-truth proxy derived from the output status time series of the same pipeline, creating a potential risk of circularity. Therefore, the reported precision and recall values should be interpreted primarily as measures of internal consistency across scenarios rather than absolute accuracy. In addition, the evaluation was limited to a single operator backbone over a six-day observation period, and its generalizability to other networks requires further investigation. ICMP measurements also provide lower precision than TWAMP or Y.1731 OAM, which require access to core network equipment. Integration with an NOC ticketing platform to obtain fully curated operational labels represents an important direction for future development.

Limitations

Four limitations should be acknowledged. First, alarm correctness was evaluated using a persistence-based ground-truth proxy derived from the output status time series of the same pipeline, which introduces a potential risk of circularity. The reported precision and recall values should therefore be interpreted primarily as measures of internal consistency across scenarios rather than as absolute accuracy. Second, packet loss resolution is limited to multiples of 20% because each probing cycle transmits five ICMP packets, so the second input to the

fuzzy engine is coarse and discrete, which constrains how finely the FOU can discriminate near the decision boundary. Third, ICMP measurements represent conditions from the probe's point of view and offer lower precision than TWAMP or Y.1731 OAM, which in turn would require access to core network equipment and therefore fall outside the external monitoring scope adopted here. Fourth, the evaluation was limited to a single operator backbone over a six-day observation period, so generalizability to other topologies, traffic characteristics, and seasonal anomalies outside this window requires further investigation.

Author Contributions

The first author was responsible for the conceptualization of the research, data collection, data analysis, and preparation of the manuscript. The second author contributed to the development of the conceptual framework, the interpretation of the research results, and the review and refinement of the manuscript. All authors have read and agreed to the final published version of the article.

REFERENCES

Adnan, R. S. A., & Kumaravel, R. (2025). A Novel Framework for Enhanced Rainfall Estimation and Forecasting Using Interval Type-2 Fuzzy Systems. *Fuzzy Information and Engineering*, *17*(1), 1–19. https://doi.org/10.26599/FIE.2025.9270050

Almeida, R. P., Ferreira, J. C., & Mendes, L. S. (2021). Fuzzy logic approaches for quality of transmission estimation in elastic optical networks. Optical Switching and Networking, 42, Article 100634. https://doi.org/10.1016/j.osn.2021.100634

Amjad, M. J., Diot, C., Konomis, D., Kveton, B., Soule, A., & Yang, X. (2021). *Optimal Probing with Statistical Guarantees for Network Monitoring at Scale*. https://doi.org/10.48550/arXiv.2109.07743

Andrade, J. R., Rocha, C., Silva, R., Viana, J. P., Bessa, R. J., Gouveia, C., Almeida, B., Santos, R. J., Louro, M., Santos, P. M., & Ribeiro, A. F. (2022). Data-Driven Anomaly Detection and Event Log Profiling of SCADA Alarms. *IEEE Access*, *10*, 73758–73773. https://doi.org/10.1109/ACCESS.2022.3190398

Chakraborty, S., et al. (2024). An effective metaheuristic based optimized type-II fuzzy inference system for fault node identification in wireless sensor network. International Journal of Communication Systems, 37(16), e5885. https://doi.org/10.1002/dac.5885

Chen, X., Liu, C. Y., Proietti, R., Li, Z., & Yoo, S. J. B. (2022). Automating Optical Network Fault Management with Machine Learning. *IEEE Communications Magazine*, *60*(12), 88–94. https://doi.org/10.1109/MCOM.003.2200110

Chen, Y., Wang, H., & Li, X. (2022). Segment-based performance monitoring and fault localization in software-defined optical networks. Journal of Optical Communications and Networking, 14(8), 612–625. https://doi.org/10.1364/JOCN.458921

Cruzes, S. (2024). Failure Management Overview in Optical Networks. *IEEE Access*, *12*, 169170–169193. https://doi.org/10.1109/ACCESS.2024.3498704

Edozie, E., Shuaibu, A. N., Sadiq, B. O., & John, U. K. (2025). Artificial intelligence advances in anomaly detection for telecom networks. *Artificial Intelligence Review*, *58*(4), 100. https://doi.org/10.1007/s10462-025-11108-x

Farheen, & Kumar, R. (2025). Sliding window-based anomaly detection. Procedia Computer Science, 258, 2520–2529.

Figueroa-García, J. C., Ramos-Cuesta, J. S., & Hernández-Pérez, G. J. (2023). On the Variance of Interval Type-2 Fuzzy Sets. *IEEE Transactions on Fuzzy Systems*, *31*(7), 2320–2330. https://doi.org/10.1109/TFUZZ.2022.3223761

Gu, J., Zhang, X., Lu, Y., Liu, P., Wang, J., Chen, M., Hu, X., Bian, Q., & Meng, Z. (2025). False alarm suppression for a distributed acoustic sensing system utilizing polarization-

time division hybrid multiplexing. Optics Communications, 592, Article 132224. https://doi.org/10.1016/j.optcom.2025.132224

IEEE. (2016). IEEE Standard for Fuzzy Markup Language. In *IEEE Std 1855-2016* (pp. 1–89). https://doi.org/10.1109/IEEESTD.2016.7479441

Joshi, R., & Garg, P. (2022). Assessing brand love, brand sacredness and brand fidelity toward halal brands. *Journal of Islamic Marketing*, *13*(4), 807–823. https://doi.org/10.1108/JIMA-04-2020-0104

Kh Altmemi, D., Adil Abdulzahra, A., & Alshawi, I. S. (2022). *A New Approach Based on an Intelligent Method to Classify Quality of Service*. https://doi.org/10.31449/inf.v46i9.4323

Kim, H. (2024). Optimal Path Calculation for Multi-ring Based Packet-Optical Transport Networks. *Journal of Web Engineering*, *23*(6), 801–812. https://doi.org/10.13052/jwe1540-9589.2364

Klinkowski, M. (2024). Dedicated Path Protection with Flexible Switching Selection in Passive Optical 5G Xhaul Access Networks *Photonics*, *11*(10). https://doi.org/10.3390/photonics11100908

Kumar, A., & Singh, R. (2024). Active probing techniques for lightpath quality assessment in DWDM transport networks. IEEE Access, 12, 14567–14582. https://doi.org/10.1109/ACCESS.2024.3356789 (

Li, H., et al. (2024). Small sample fiber full state diagnosis based on fuzzy clustering and improved ResNet network. IET Signal Processing, 2024, Article 5512014. https://doi.org/10.1049/2024/5512014

Li, M., Yang, M., & Chen, P. (2023). Alarm reduction and root cause inference based on association mining in communication network. *Frontiers in Computer Science*, *5*. https://doi.org/10.3389/fcomp.2023.1211739

Li, X., Lou, S., Gao, W., Guo, Y., & Wang, X. (2025). Disturbance event identification and localization based on temporal convolutional network (TCN) and sliding window algorithm. Proceedings of SPIE, 13654, Article 136540N. https://doi.org/10.1117/12.3059143

Manias, D. M., Javadtalab, A., Naoum-Sawaya, J., & Shami, A. (2023). The Role of Optical Transport Networks in 6G and Beyond: A Vision and Call to Action. *Journal of Sensor and Actuator Networks*, *12*(3). https://doi.org/10.3390/jsan12030043

Mayr, C., Risso, C., & Grampín, E. (2021). Crafting optimal and resilient iBGP-IP/MPLS overlays for transit backbone networks. *Optical Switching and Networking*, *42*, 100635. https://doi.org/10.1016/J.OSN.2021.100635

Mendel, J. M. (2024). *Explainable Uncertain Rule-Based Fuzzy Systems* (3rd Edition). https://doi.org/10.1007/978-3-031-35378-9

Miranda, G., MacEdo, D. F., & Marquez-Barja, J. M. (2022). Estimating Video on Demand QoE From Network QoS Through ICMP Probes. *IEEE Transactions on Network and Service Management*, *19*(2), 1890–1902. https://doi.org/10.1109/TNSM.2021.3129610

Rainio, O., Teuho, J., & Klén, R. (2024). Evaluation metrics and statistical tests for machine learning. *Scientific Reports*, *14*(1), 6086. https://doi.org/10.1038/s41598-024-56706-x

Reyes, R. R., Esati, S., & Bauschert, T. (2021). Traffic Protection in Multilayer Core Networks by Optimum Thinning of MPLS Tunnel Capacities. *2021 International Conference on Optical Network Design and Modeling (ONDM)*, 1–6. https://doi.org/10.23919/ONDM51796.2021.9492463

Rodríguez-Ramos, A., da Silva Neto, A. J., & Llanes-Santiago, O. (2024). An improved fault diagnosis scheme based on a type-2 fuzzy classification algorithms. In Lecture Notes in Computer Science (pp. 95–108). Springer. https://doi.org/10.1007/978-3-031-49552-6_8

Şahin, İ., & Ulu, C. (2023). Altitude control of a quadcopter using interval type-2 fuzzy controller with dynamic footprint of uncertainty. *ISA Transactions*, *134*, 86–94. https://doi.org/10.1016/J.ISATRA.2022.08.020

Shukla, P., Majhi, G., & Kumar, Y. (2024). Proactive fault localization and alarm correlation in DWDM networks. Asian Journal for Convergence in Technology (AJCT), 10(1), 14–18. https://doi.org/10.33130/AJCT.2024v10i01.003

Sica, M., Patri, S., Safari, P., Rai, V., John, J., Shariati, B., Fischer, J. K., & Freund, R. (2026). Detection, identification, and localization of faults in PONs using joint OLT and OTDR telemetry data. Journal of Optical Communications and Networking, 18(9), D44–D55. https://doi.org/10.1364/JOCN.587134

Simanjuntak, I. U. V, Larasati, S., Rahmawati, Y., & Santika, D. A. (2022). Modernization of Dense Wavelength Division Multiplexing (DWDM) Route Surabaya-Bangil to Increase Optical Network Capacity. *ELKHA: Jurnal Teknik Elektro*, *14*(2), 89. https://doi.org/10.26418/elkha.v14i2.56003

Tan, Y., Yuan, X., Li, X., et al. (2026). Fault detection filter design for IT2 fuzzy systems with DE-WTOD protocols. International Journal of Control, Automation and Systems, 24, 602–613. https://doi.org/10.1007/s12555-026-00044-3

Wang, D., Zhang, C., Chen, W., Yang, H., Zhang, M., & Lau, A. P. T. (2022). *A Review of Machine Learning-based Failure Management in Optical Networks*. http://arxiv.org/abs/2208.10677

Wang, Y., Zhang, C., Li, J., Pang, Y., Zhang, L., Zhang, M., & Wang, D. (2024). AlarmGPT: An intelligent alarm analyzer for optical networks using a generative pre-trained transformer. Journal of Optical Communications and Networking, 16(6), 681–694. https://doi.org/10.1364/JOCN.521913

Wu, D., & Mendel, J. (2019). *Recommendations on Designing Practical Interval Type-2 Fuzzy Systems*. http://arxiv.org/abs/1907.01697

Wu, Z., Li, X., & Ma, S. (2026). Protocol-based fault detection for interval type-2 fuzzy systems under resilient memory event-triggered mechanism against DoS attacks. Transactions of the Institute of Measurement and Control. https://doi.org/10.1177/01423312261418073

Xie, C., & Zhang, B. (2022). Scaling Optical Interconnects for Hyperscale Data Center Networks. *Proceedings of the IEEE*, *110*(11), 1699–1713. https://doi.org/10.1109/JPROC.2022.3178977

Xing, C., Zhang, C., Zhang, M., Fan, Y., Jiang, X., Bi, Z., Xiong, J., & Wang, D. (2025). Alarm priority sorting with multimodal data fusion in optical networks. In Optical Fiber Communication Conference (OFC) 2025

Zhao, Y., Lin, Y., Li, Y., Zhang, D., Liu, Y., Zheng, Y., Wang, D., Liu, S., Cao, S., Feng, H., Li, H., & Liu, X. (2024). Multi-layer resource scheduling architecture and algorithm for a service-oriented optical network based on a fine grain OTN. *Journal of Optical Communications and Networking*, *16*(10), F13–F25. https://doi.org/10.1364/JOCN.527736

Zhou, L., Zhang, M., & Liu, Q. (2023). Quality of transmission-aware routing and monitoring strategies in dynamic DWDM networks. Optical Fiber Technology, 75, Article 103198. https://doi.org/10.1016/j.yofte.2023.103198